SANDIA REPORT
SAND2006-7269
Unlimited Release
Printed November 2006

Active Resonant Subwavelength Grating for Scannerless Range Imaging Sensors

Shanalyn A. Kemme, David W. Peters, Robert R. Boye, and Robert O. Nellums

Prepared by
Sandia National Laboratories
Albuquerque, New Mexico 87185 and Livermore, California 94550

Sandia is a multiprogram laboratory operated by Sandia Corporation,
a Lockheed Martin Company, for the United States Department of Energy's
National Nuclear Security Administration under Contract DE-AC04-94AL85000.

Issued by Sandia National Laboratories, operated for the United States Department of Energy by Sandia Corporation.

Available to DOE and DOE contractors from
U.S. Department of Energy
Office of Scientific and Technical Information
P.O. Box 62
Oak Ridge, TN 37831

Telephone: (865) 576-8401
Facsimile: (865) 576-5728
E-Mail: reports@adonis.osti.gov
Online ordering: http://www.osti.gov/bridge

Available to the public from
U.S. Department of Commerce
National Technical Information Service
5285 Port Royal Rd.
Springfield, VA 22161

Telephone: (800) 553-6847
Facsimile: (703) 605-6900
E-Mail: orders@ntis.fedworld.gov
Online order: http://www.ntis.gov/help/ordermethods.asp?loc=7-4-0#online

SAND 2006-7269
Unlimited Release
Printed November 2006

Active Resonant Subwavelength Grating for Scannerless Range Imaging Sensors

Shanalyn A. Kemme and Robert R. Boye,
Photonic Microsystems Technologies

David W. Peters
Applied Photonic Systems

Robert O. Nellums
EO Imaging Technology

Sandia National Laboratories
P.O. Box 5800 M/S 1082
Albuquerque, NM 87185-1082

Abstract

In this late-start LDRD, we will present a design for a wavelength-agile, high-speed modulator that enables a long-term vision for the THz Scannerless Range Imaging (SRI) sensor. It takes the place of the currently-utilized SRI micro-channel plate which is limited to photocathode sensitive wavelengths (primarily in the visible and near-IR regimes).

Two of Sandia's successful technologies – subwavelength diffractive optics and THz sources and detectors – are poised to extend the capabilities of the SRI sensor. The goal is to drastically broaden the SRI's sensing waveband – all the way to the THz regime – so the sensor can see through image-obscuring, scattering environments like smoke and dust. Surface properties, such as reflectivity, emissivity, and scattering roughness, vary greatly with the illuminating wavelength. Thus, objects that are difficult to image at the SRI sensor's present near-IR wavelengths may be imaged more easily at the considerably longer THz wavelengths (0.1 to 1mm).

The proposed component is an active Resonant Subwavelength Grating (RSG). Sandia invested considerable effort on a passive RSG two years ago, which resulted in a highly-efficient (reflectivity greater than gold), wavelength-specific reflector. For this late-start LDRD proposal, we will transform the passive RSG design into an active laser-line reflector.

Table of Contents

Table of Figures

Introduction

In this late-start LDRD, we will present a design for a wavelength-agile, high-speed modulator that enables a long-term vision for the THz Scannerless Range Imaging (SRI) sensor. It takes the place of the currently-utilized SRI micro-channel plate which is limited to photocathode sensitive wavelengths (primarily in the visible and near-IR regimes).

The proposed component is an active Resonant Subwavelength Grating (RSG). Sandia invested considerable effort on a passive RSG two years ago, which resulted in a highly-efficient (reflectivity greater than gold), wavelength-specific reflector. For this late-start LDRD proposal, we will transform the passive RSG design into an active laser-line reflector.

Two of Sandia's successful technologies – subwavelength diffractive optics and THz sources and detectors – are poised to extend the capabilities of the SRI sensor. The goal is to broaden drastically the SRI's sensing waveband – all the way to the THz regime – so the sensor can see through image-obscuring, scattering environments like smoke and dust. Surface properties, such as reflectivity, emissivity, and scattering roughness, vary greatly with the illuminating wavelength. Thus, objects that are difficult to image at the present SRI sensor's near-IR wavelengths may be imaged more easily at the considerably longer THz wavelengths (0.1 to 1mm).

SRI sensing is a flagship technology that Sandia has developed. Sandia's successful applications of SRI sensors range from underwater imaging in turbidity for the Navy's Coastal Systems Station, to structural dynamics measurements and space vehicle inspection for NASA's International Space Station. Clearly, Sandia has thrived with each SRI sensor delivery; and every field installment benefits from a multitude of evolutionary engineering improvements. However, to continue on this successful path Sandia must take the opportunity to develop fundamental, disruptive technologies and apply them to systems such as the SRI sensors. This RSG demonstration is key to significantly advancing the SRI sensor family.

Passive Resonant Subwavelength Grating (RSG)

The resonant subwavelength grating (RSG) is an optical device with a resonant reflection characteristic due to the interaction of a subwavelength grating and waveguide [1]. In contrast to other waveguide devices, the waveguide is not used for propagating the signal; the device is used as a free space component, as shown in Figure 1. To prevent losing power to propagating diffracted orders of the grating, a subwavelength period is employed. The period of the grating allows for a single propagating order within the higher refractive index of the waveguide. When the incident angle, polarization, and wavelength are correct, this diffracted order overlaps with an allowed mode of the waveguide, resulting in a resonant reflection similar to the measured responses shown in Figure 2 [2].

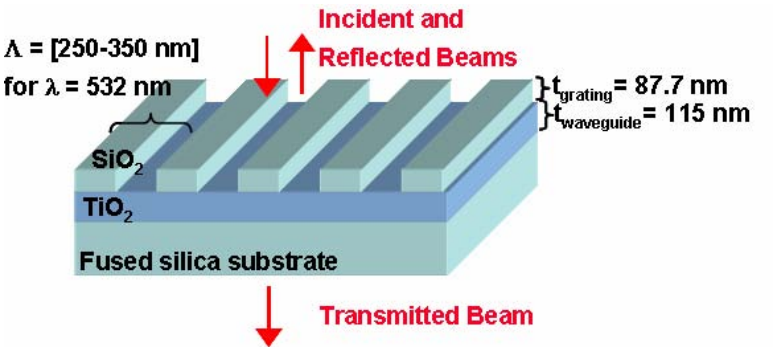

Figure 1 Layout of a resonant subwavelength grating (RSG).

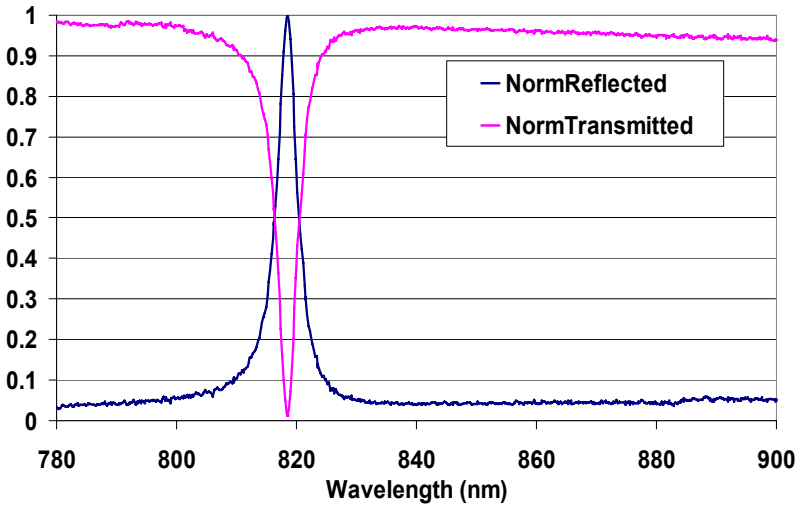

Figure 2 Measured resonant reflection and transmission of an RSG.

Active Resonant Subwavelength Grating Design Considerations

Design considerations for the active RSG are interdependent and sometimes conflicting. The resonant conditions of the RSG predict 100% reflections and 0% transmission at the design wavelength. This is not an approximation, but a direct consequence of the non-absorbing dielectric materials in the component. The device is extremely sensitive to changes in the index of refraction, primarily in the waveguide region, so that this presents a path to an active device.

There are several mechanisms for refractive index variation in a dielectric. The linear electro-optic effect relies on a material with a non-centrosymmetric structure. A randomly oriented, amorphous film will not show a coherent response. With this effect, the application of biasing potential will change the refractive index, causing a shift of the resonance peak spectrum. We could also utilize the quadratic electro-optic effect with the same electric field application. And alternative to the electro-optic effect would be the use of non-linear optical materials. Here, an optical pump input induces a change in the refractive index. A separate probe input optical beam senses the shift in resonant response of the RSG. Fundamentally, this option is sound, but

realizing this configuration is somewhat more difficult. The pump beam is generally within the detection band of the system and can be high power. For this reason, the pump beam must be separated (filtered) from the signal or it contributes to noise.

Utilizing the electro-optic effect would be an elegant packaging solution that could be integrated into the component for a high-speed device response. However, this now requires that we introduce absorbing materials into the component that will reduce the high optical contrast and obscure the optical input and output signal. The need to minimize the biasing voltage of the device while maximizing both the input and output optical signals presents a trade-off. Finally, the design wavelength constrains the available material set. Here, we intend the design wavelength to center around 850nm, which is the current operating wavelength of the SRI, and generally in the visible for testing ease.

For our work using the linear electro-optic mechanism, we assume that the incident optical signal is not of such high irradiance that it induces a change in the refractive index. Also, we are employing linear modeling codes, such as Rigorous Coupled Wave Analysis to predict the optical response as a function of waveguide index.

Figure 3 shows the cross-section of an RSG design [3] utilized in the analysis on an active component around an incident, visible wavelength of 638.6 nm. The predicted transmitted and reflected resonances are shown in Figure 4 for a normally incident beam with TE polarization, as a function of input wavelength. The resonance is quite narrow due to the small refractive index contrast between the waveguide and the surrounding regions.

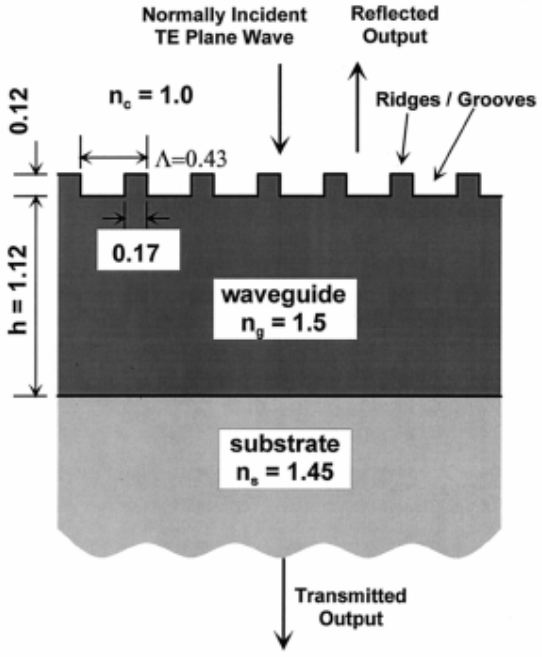

Figure 3 RSG design used for the below analysis. The input light is a normally incident TE wave. All dimensions are in micrometers [3].

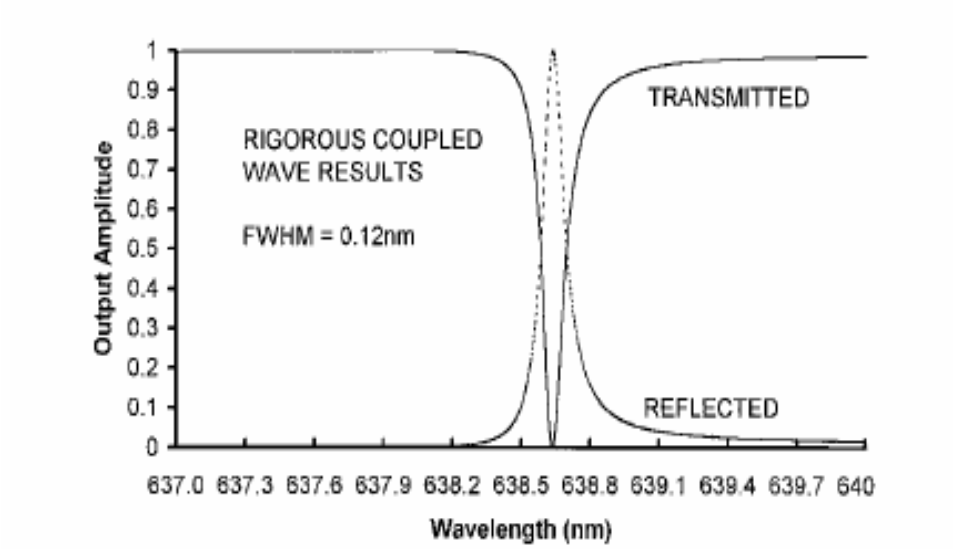

Figure 4 RCWA shows the resonance of the device assuming a constant refractive index. The resonant wavelength does not exactly match the wavelength of minimum reflectance resulting from the effective AR coating provided by the grating [3].

If the incident wavelength in the above design is fixed at 638.4 nm and the refractive index of the waveguide material is varied, the predicted reflection and transmission responses are shown in Figure 5. Note that a change of less than 0.0008 in the refractive index varies the response 100%.

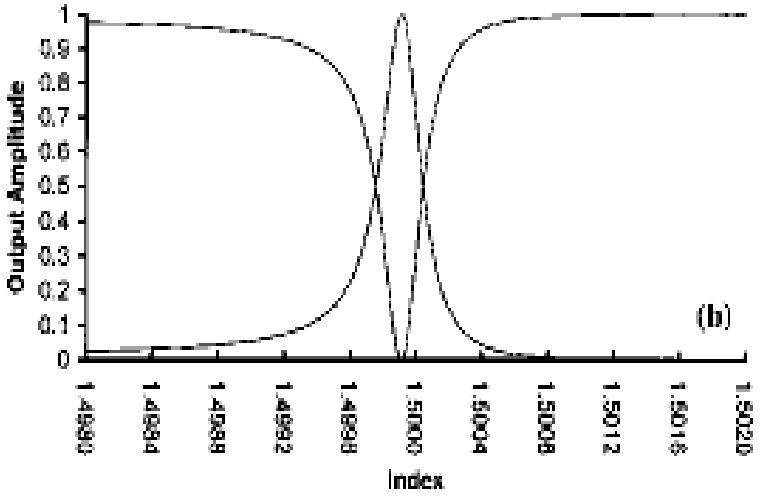

Figure 5 A small change of waveguide index causes dramatic change in output as resonance peak shifts. Data shown below assumes constant wavelength at 638.4 nm [3].

Previous Work on Active RSGs

Figure 6 shows the device layout for an active RSG modulator [4]. This semiconductor-based device is for an incident Near-IR wavelength of 1.55 microns.

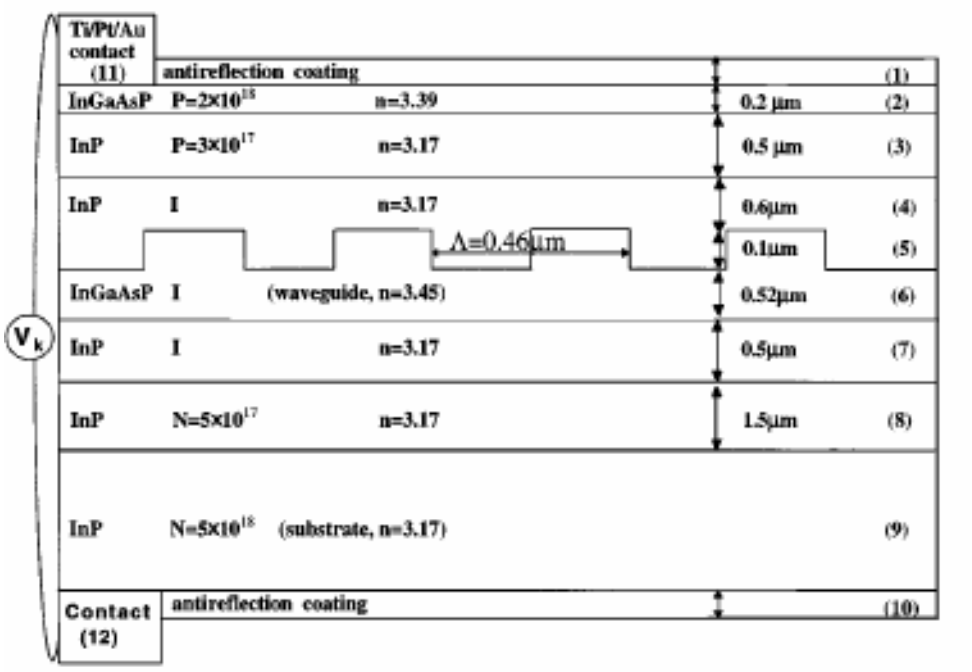

Figure 6 Active RSG device design in InP/InGaAsP semiconductor materials [4].

The input, ac driving voltage of 5V and the resulting measured reflectance modulation is shown in Figure 7. The device speed is not optimal as the electrode layout contains significant capacitance. On the other hand, the framed electrode configuration has the advantage of not obscuring the input or reflected optical signals.

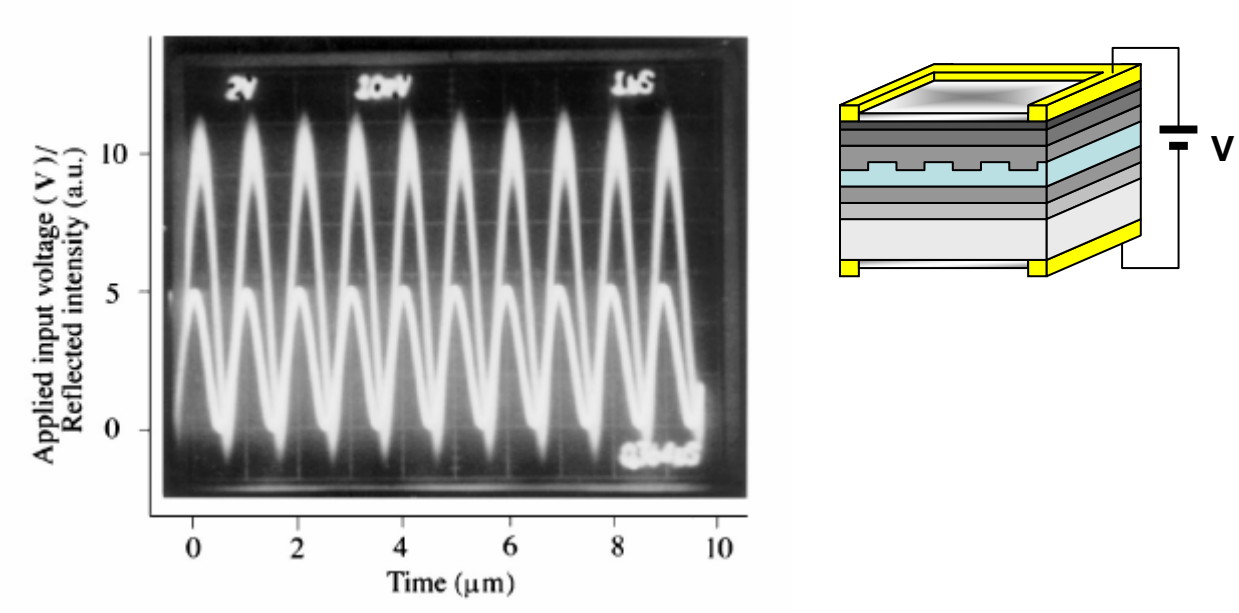

Figure 7 Reflection intensity response to an externally applied modulated voltage. The upper curve is the reflected intensity in arbitrary units. The lower curve is the applied voltage of 5V ac in reverse bias. The electrode configuration with respect to the RSG semiconductor device is shown on the right [4].

The following figures show simulation work published [5] using PLZT (Lead Lanthanum Zirconate Titanate) for the waveguide material and an interdigitated electrode configuration for greater field strength in the waveguide region, see Figure 8. The grating/electrodes were Indium Tin Oxide (ITO), which is an almost transparent conducting material. While this introduces some absorption into the RSG, and thus reduces the resonant effect, it presents less of an obscuration to both the incident and the reflected signals.

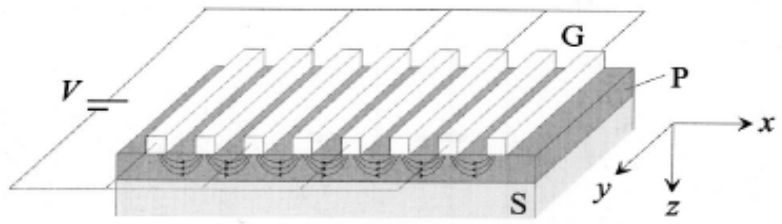

Figure 8 Concept of the RSG. G denotes the ITO, comb-shaped grating electrodes. P is the PLZT waveguide layer, and S is the sapphire substrate [5].

Figure 9 shows the material design parameters in the RSG cross-section. The refractive index of the PLZT is modulated as the bias voltage ranges from 0V to 6V. The predicted reflectance as a function of wavelength is shown in Figure 10.

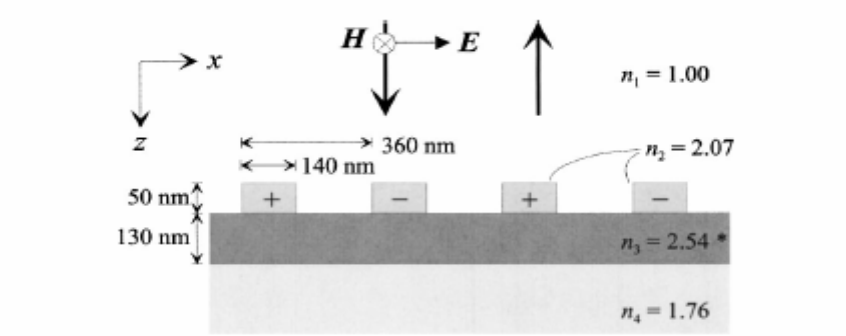

Figure 9 Material design parameters for the PLZT-based active RSG [5]. Refractive indices are for air (n_1), ITO (n_2), PLZT at zero bias potential (n_3), and sapphire (n_4).

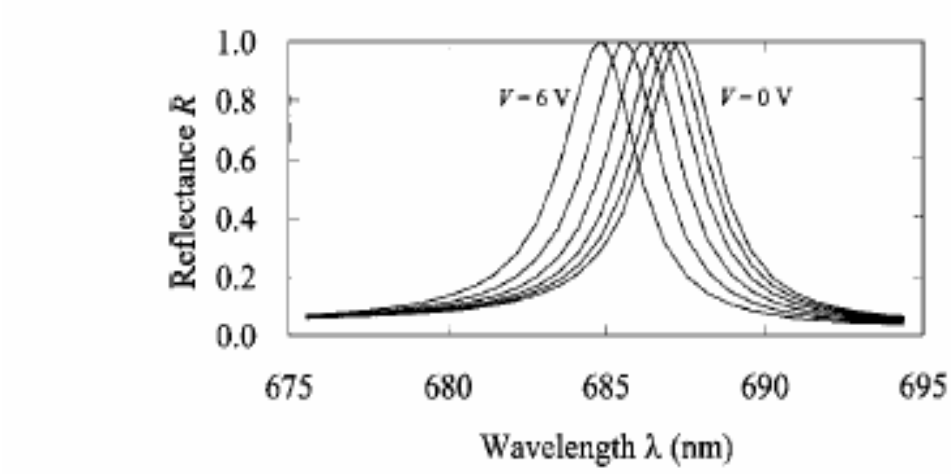

Figure 10 Predicted reflection spectra for the proposed device. The spectra, from right to left, are for these bias potentials: V=0, 2, 3, 4, 5, and 6V.

Possible Materials for Linear E-O

- LiNbO3 (lithium niobate, ne ~ 2.2, no ~ 2.3) –
  - Well understood waveguide fabrication (Ti in-diffusion or proton exchange)
  - High EO coefficient
  - Extremely narrow resonance for in-diffused guides
- LiTaO3 (lithium tantalate) – better UV transmission (280 nm) than LiNbO3
- KTP potassium titanyl phosphate
- BBO (barium metaborate, ne ~ 1.66, no ~ 1.56) –
  - Good UV transmission
  - Typically used in bulk form for NLO applications
  - Waveguide fabrication done using H+ or He implantation
- BaTiO3 (ne ~ 2.28, no ~ 2.32) - barium titanate, Extremely high EO coefficient
- PLZT (n ~ 2.3) Lead Lanthanum Zirconate Titanate
  - High linear and quadratic EO coefficient
  - Can be deposited using laser assisted deposition or sol-gel based process
  - High index provides good resonance peak

Active RSG Material Survey and Simulations

We investigated various methods for the realization of an active RSG. A promising option is the incorporation of a material with an index of refraction that we can vary with voltage: an electro-optic material. We then considered which materials and configurations we could use in such a device as well as the electrode geometry.

Linear electro-optic materials allow us to vary the refractive index with the application of an electric field. We considered materials that exhibit a strong electro-optic effect, have low-loss in the wavelength range of interest, and are compatible with the fabrication steps required for the RSG process. Candidate materials are lithium niobate ($LiNbO_3$), lithium tantalite ($LiTaO_3$), potassium titanyl phosphate (KTP), barium metaborate (BBO), barium titanate ($BaTiO_3$), and lead lanthanum zirconium titanate (PLZT).

Candidate electrode geometries are frames for applying the voltage, interdigitated electrode fingers, or a combination. Frames offer the advantage of keeping the optical transmission portion of the device free of all optically-absorbing electrical regions, maximizing the optical performance. This approach requires higher voltages to obtain the field strength required in the waveguide region as a result of the non-centralized location of the electrodes. Interdigitated electrodes inside the optical area of the device can reduce by orders of magnitude the distance between electrodes and thus reduces the required voltage by a similar amount. Interdigitated electrodes will interfere with the optical properties due to their location in the optical path.

We explored various geometries of $BaTiO_3$ guiding layers on a silicon dioxide substrate. Grating materials consisting of silicon dioxide (SiO_2), $BaTiO_3$, indium tin oxide (ITO), and combinations of these were considered. The higher-index $BaTiO_3$ creates a wider wavelength

resonant peak than the lower-index silicon dioxide. ITO offers a conductive, mostly transparent material for electrical connections with active control of the device response. However, ITO is lossy, which could detrimentally affect device performance.

Directly etching a grating into a $BaTiO_3$ layer would provide a guiding layer and grating layer of the same material. This straightforward approach results in a broad (20.5nm FWHM) reflection peak as seen in Figure 11. The reflectivity in the main peak reaches a value of 100% as the materials used in the simulation are assumed lossless in this wavelength range. The reflectivity outside the main peak can be lowered by adjusting the grating and guiding layer thicknesses. For these simulations these adjustments were not made. It should be noted that these reflectivity values could be lowered with additional design effort.

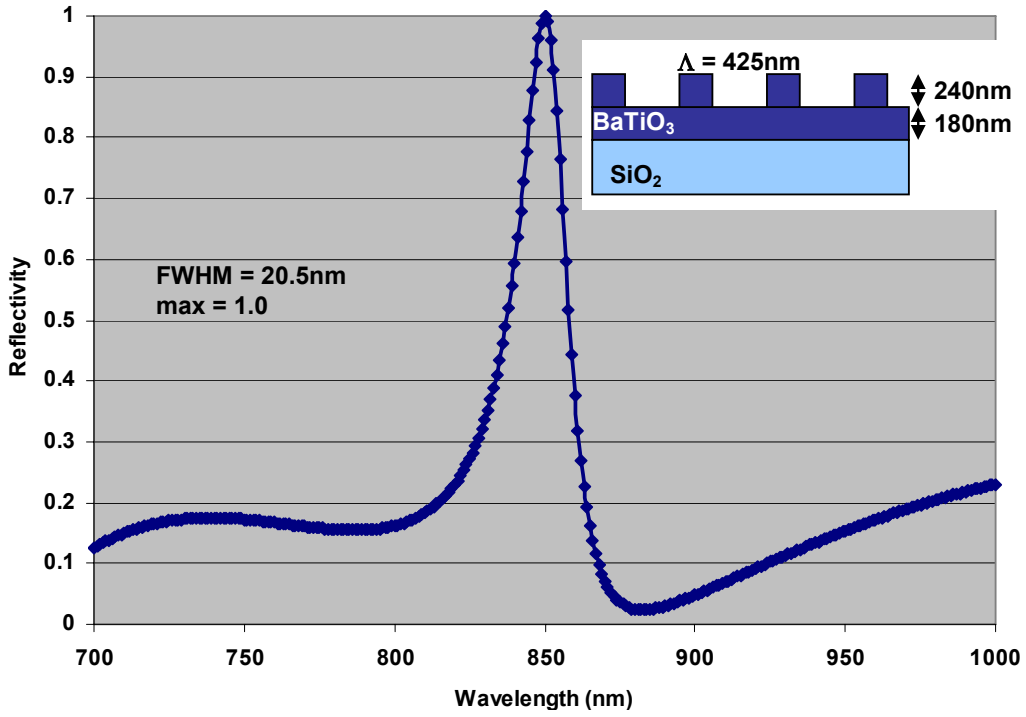

Figure 11 Reflectivity of an RSG with a $BaTiO_3$ guiding layer and $BaTiO_3$ grating layer.

The width of the reflection peak is dramatically affected by the material used in the grating layer. Switching this layer from the high-index $BaTiO_3$ to a lower-index silicon dioxide (n = 1.45) narrows the reflection peak from 20.5nm to 1.2nm as seen in Figure 12. Device parameters are slightly altered to maintain the center of the reflectivity peak at 850nm.

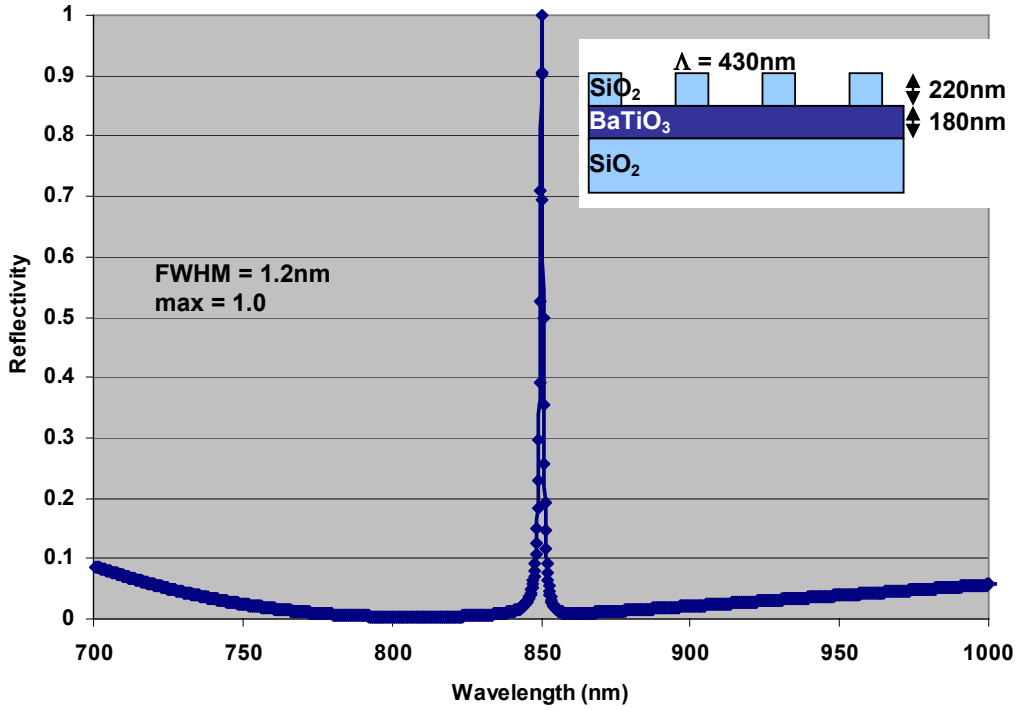

Figure 12 Reflectivity of an RSG with a $BaTiO_3$ guiding layer and SiO_2 grating layer.

Use of interdigitated electrodes would require incorporation of electrodes in the optically-active region of the device. Indium tin oxide (ITO) is commonly used for such applications because it is mostly transparent. The imperfect transparency is the result of a nonzero imaginary component of the refractive index. To ascertain the effect of the imaginary component on device performance we can model an RSG using the refractive index of ITO, with the imaginary component set to zero (n = 1.9) and for the actual material (n = 1.9 + 0.005i). The difference in the response is clear when comparing Figure 13 to Figure 14. The addition of the imaginary component to the refractive index results in a dropping of the peak reflectivity from 1.0 to 0.93. Otherwise, the responses are similar, with a minimal shift in the reflection peak and a slight widening of the main lobe.

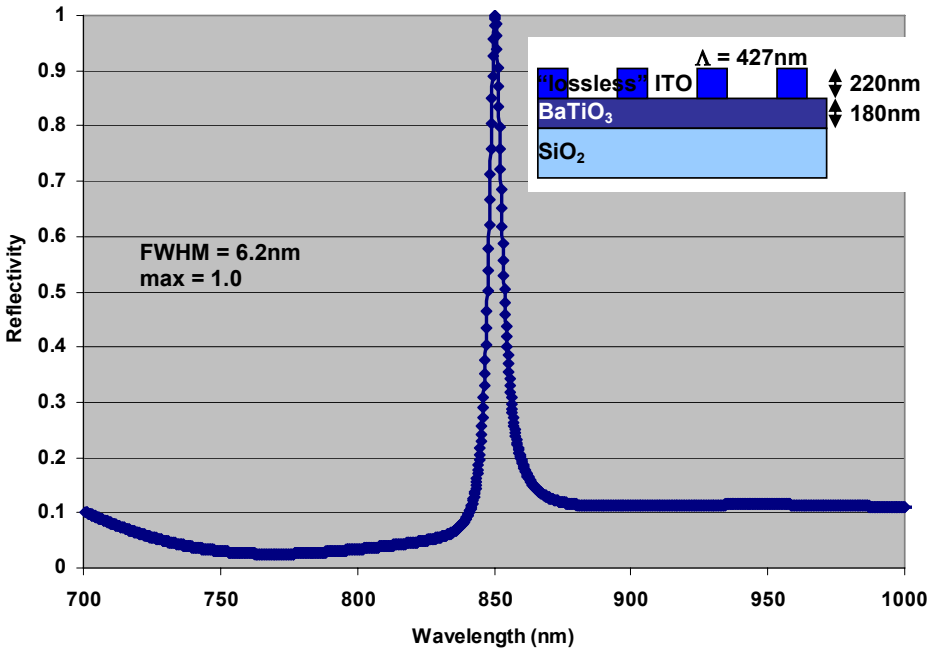

Figure 13 Reflectivity of an RSG with a $BaTiO_3$ guiding layer and a "lossless ITO" grating layer.

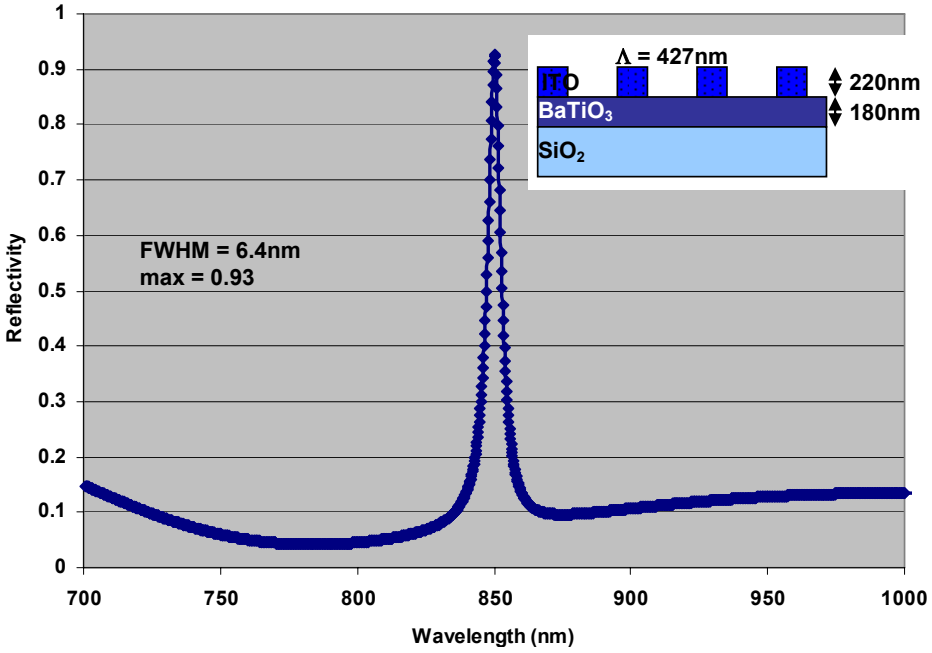

Figure 14. Reflectivity of an RSG with a $BaTiO_3$ guiding layer and an ITO grating layer.

To avoid the absorption evident in Figure 14, a dual-layer grating can distance the lossy ITO from the high electric fields present in the guiding layer. The lower layer of the grating may be either the low-index SiO_2, or the high-index $BaTiO_3$. Figure 15 shows the results of the numerical simulation for the SiO_2 case. This configuration is similar to that of Figure 12, with

the addition of the ITO layer. Similar to the earlier case with a low-index grating layer, the reflection peak is quite narrow. The addition of the SiO_2 to the grating layer ameliorates the effect of the lossy ITO, with only 1% absorption seen at the peak rather than the 7% seen with the wholly ITO grating layer.

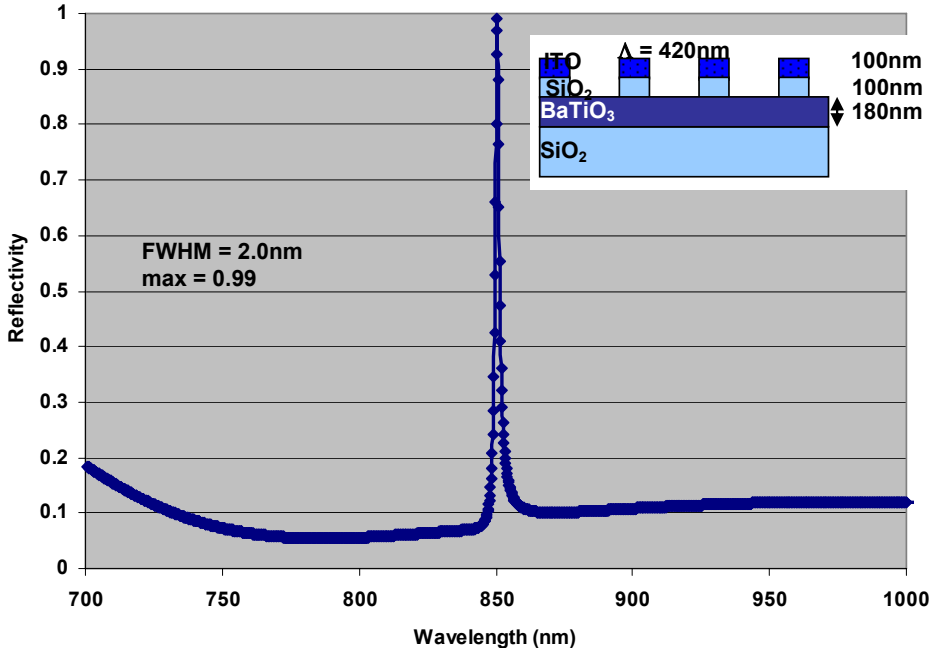

Figure 15 Reflectivity of an RSG with a $BaTiO_3$ guiding layer and an ITO/SiO_2 grating layer.

Similarly, we can create a dual-layer grating using ITO and $BaTiO_3$. With the higher-index material now incorporated into the grating the reflection peak broadens to 20nm as shown in Figure 16.

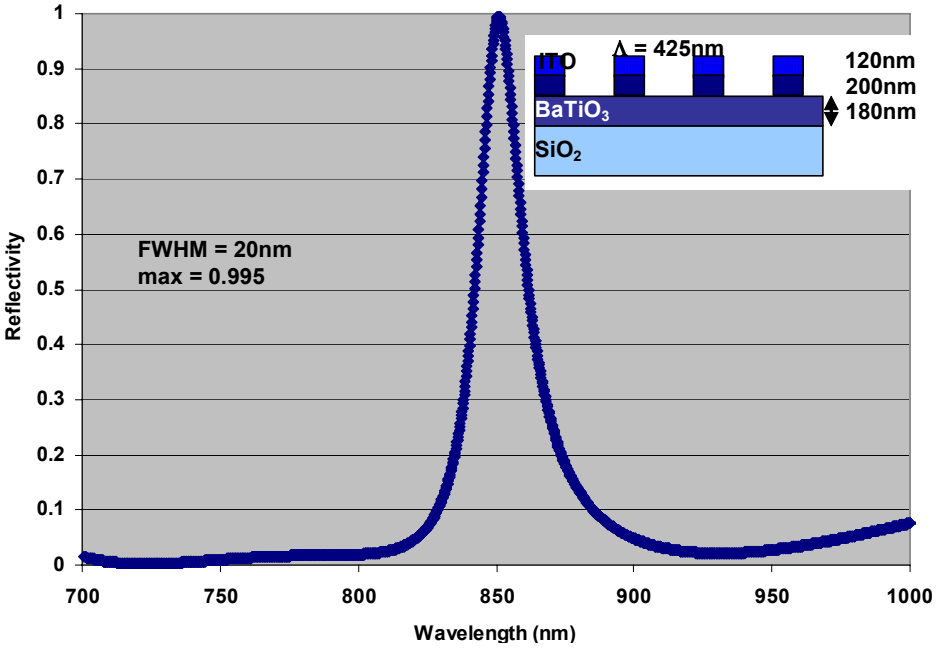

Figure 16. Reflectivity of an RSG with a $BaTiO_3$ guiding layer and an ITO/SiO_2 grating layer.

An RSG is typically considered a reflectance-based component. This is because, for wide spectral band incident light, only a narrow notch will be returned with large contrast. However, often a reflectance-based optical configuration is problematic. Either the input signal is obscured by the detecting device, or a beamsplitter is necessary to allow the signal to propagate along an alternate detecting path.

In this application, we can utilize the active RSG in the transmissive mode. Here, all light passes straight through except for the small notch around the resonant wavelength. The illuminating source for the SRI is a narrowband laser; essentially a single wavelength. Thus we may utilize one steep side of the transmittance notch and measure the modulated return signal as the notch shifts with bias voltage. Figure 17 shows the transmission characteristic, as a function of wavelength for the above RSG device with a $BaTiO_3$ guiding layer and an ITO/SiO_2 grating layer.

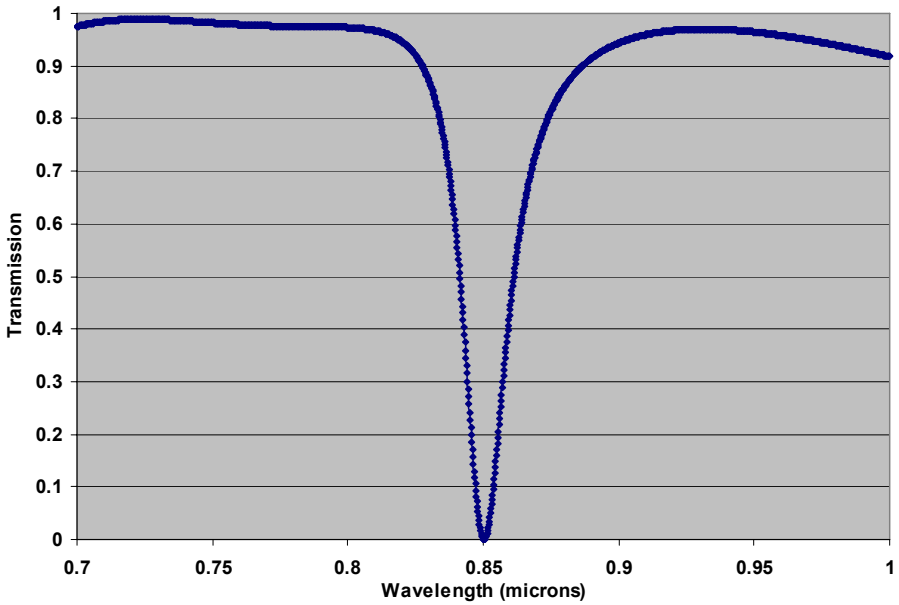

Figure 17 Transmissivity of an RSG with a $BaTiO_3$ guiding layer and an ITO/SiO_2 grating layer.

Electrode Configurations

A straightforward way to modulate the RSG is to vary the refractive index of one of the regions; specifically, the waveguide region. An applied field can induce a refractive index change through the electro-optic effect. Two possible configurations for the electrodes are shown in Figure 18. The field may be applied across the surface of the device with interdigitated electrodes or through the depth of the structure by applying electrodes atop the grating mesas and to the lower surface of the device.

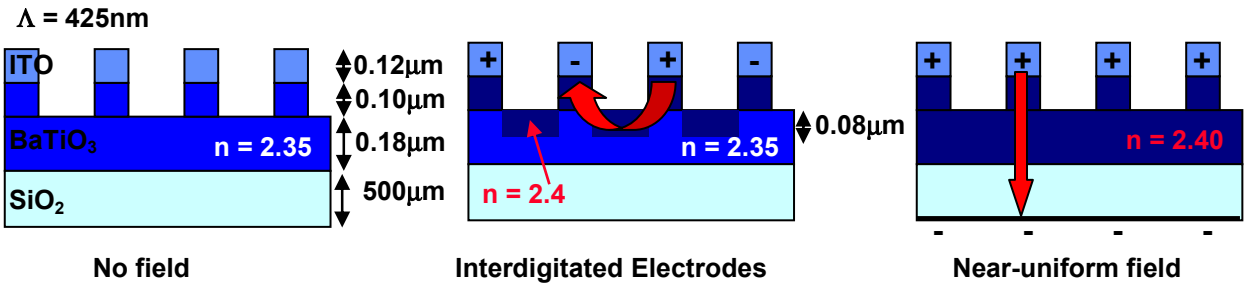

Figure 18 Side view of RSG showing effect of interdigitated top-side electrodes and bottom-contact electrodes.

The interdigitated electrodes have the advantage of minimal interference with the optical path; however the electric field is nonuniform in the guiding region. In the case of a lower electrode the field is more uniform in the region of the $BaTiO_3$. Here the electrodes are much further apart (note that the SiO_2 substrate is not drawn to scale). This thickness necessitates a much higher voltage difference to achieve the same electric field strength. For $3x10^7$V/m the interdigitated configuration would require on the order of 15V, while the back-side option, with the indicated substrate thickness, would require 15000V. We can make rough approximations of the refractive index of the $BaTiO_3$ material in the two configurations. The darker regions in Figure 18 show regions where the refractive index is increased by 0.05 by the applied electric field. The effect on the transmission is shown in Figure 19. The blue dotted line indicates a single wavelength whose transmission ranges from near zero to greater than 85% with the application of an electric field.

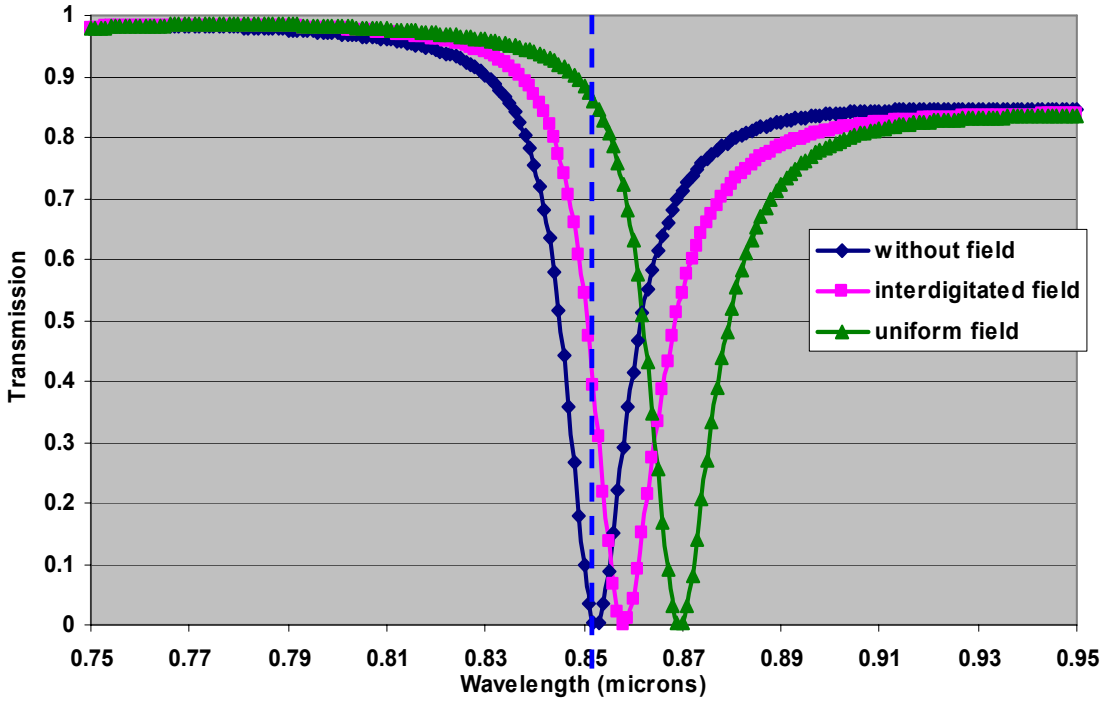

Figure 19 Transmissivity for three electrode configurations. The dotted line highlights the high contrast in signal transmission, from near zero with no field applied to greater than 85%, with an applied field.

Conclusions and Initial Plans for Further Work

We conclude with the next steps to demonstrate this device. Starting with the PLZT device design presented in Ref [5] we used RCWA to look at various design options using a PLZT waveguide. We replaced the ITO electrodes with gold. This results in a much wider resonance, but it facilitates fabrication significantly. However, only one transition may be sharp enough to be useful. We introduced a buffering dielectric layer between the PLZT and the gold electrodes in an attempt to isolate the absorbing gold from the high-field waveguide region and reduce the minimum signal level. Illuminating with an off-axis beam provides fairly sharp transitions as shown in Figure 20 and Figure 21.

These two cases assumed different indices for the PLZT (published results have varied widely). The transmission curves allow for large output signal contrasts with minima less than 1% and peaks greater than 95%. Using a published design prediction as an initial guide [5] to the required biasing potential and increasing this slightly to account for the intervening dielectric buffer layer, the voltage necessary may be 40 V for full modulation. We will watch for signs of breakdown at the material surface across the small space (~200nm) between electrodes.

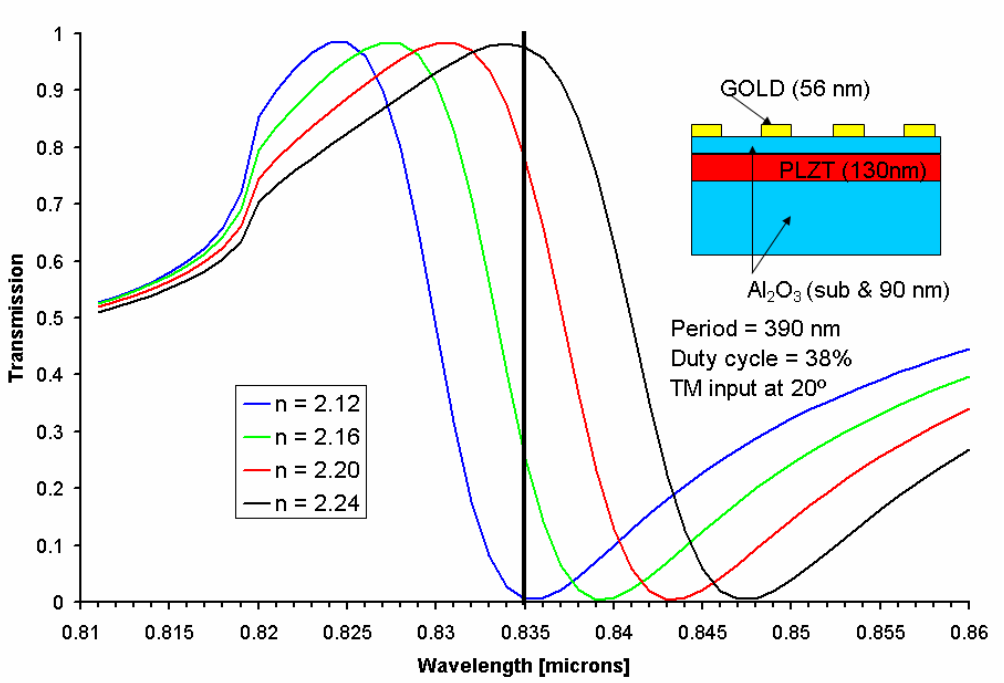

Figure 20 Transmission transition around 835 nm for the configuration in the inset. A change in refractive index, induced by the applied biasing potential, of 0.12 will cause the transmitted signal to vary from 1% to 95%. The input signal has a TM polarization (polarization vector perpendicular to the grating lines).

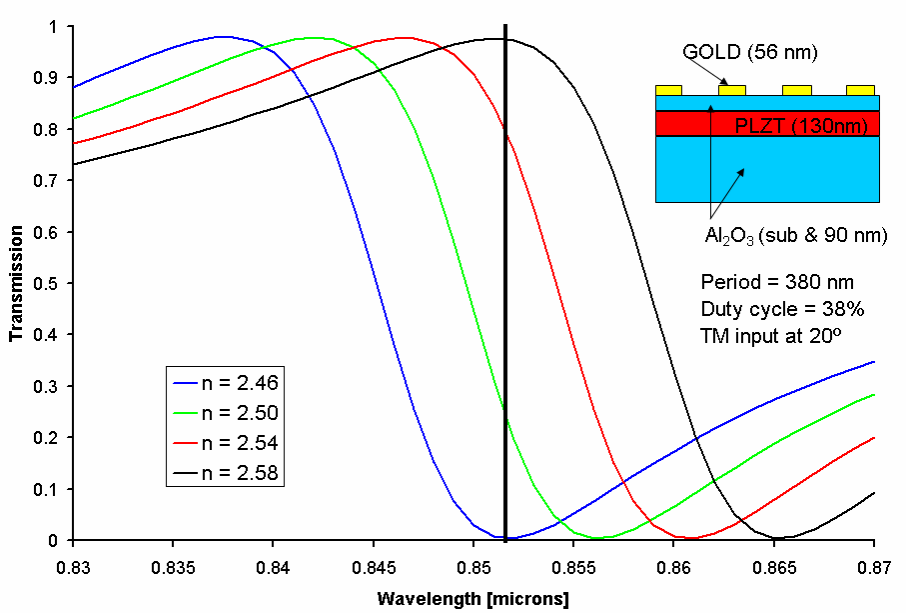

Figure 21 Transmission transition around 857 nm for the configuration in the inset. Here we use other, published refractive index values for PLZT. A change in refractive index, induced by the applied biasing potential, of 0.12 will cause the transmitted signal to vary from 1% to 95%. The input signal has a TM polarization (polarization vector perpendicular to the grating lines).

For the SRI application, the crucial requirement is to gain modulate the intensity of the return at a frequency of 10 to 200 MHz, prior to focusing the return onto the detector image plane. With the RSG, gain modulation is achieved by varying the dielectric index in and out of resonance at the wavelength of operation. This is most readily done in the transmission mode, by inserting the RSG between the lens aperture and the detector focal-plane. This requires that the RSG active area be sufficient to avoid vignetting, that similar gain modulation occurs over a range of acceptance angles, and that polarization of the incident light is compatible with the RSG.

If this concept is feasible, it will immediately advance the SRI state-of-the-art in 4 areas. First, the RSG has potential to provide modulation to the detector focal plane with less image blur or aberration than can currently be achieved using the current image-intensifier technology. Second, it will provide for the first time, a potentially low-cost means for modulation, enabling a new range of low-cost applications. Third, the amount of drive power for the modulator is substantially reduced, because the required voltages are reduced from hundreds of Volts to only about 5 Volts. Finally, the application of the RSG can be extended into the infrared and THz bands, well beyond the capability of intensifier tube technology

References

1. S.S. Wang, R. Magnusson, J.S. Bagby and M.G. Moharam, "Guided-mode resonances in planar dielectric-layer diffraction gratings," J.Opt.Soc.Am. A vol. 7, 1464-1474 (1990).

2. Shanalyn A. Kemme, David W. Peters, Joel R. Wendt, Tony R. Carter, Sally Samora, G. Ronald Hadley, Mial E. Warren and Carter L. Grotbeck, "Arrayed Resonant Subwavelength Gratings LDRD 38618 Final Report", SAND Report 2003-4115 (2003).

3. . Robert R. Boye, Richard W. Ziolkowski, and Raymond K. Kostuk, "Resonant waveguide-grating switching device with nonlinear optical material," Applied Optics, vol. 38, no. 24, 5181-5185 (1999).

4. A. Sharon, D. Rosenblatt, A.A. Friesem, H.G. Weber, H. Engel, and R. Steingrueber, "Light modulation with resonant grating-waveguide structures," Optics Letters, vol. 21, no. 19, 1564-1566, (1996).

5. Hiroyuki Ichikawa and Hisao Kikuta, "Dynamic guided-mode resonant grating filter with quadratic electro-optic effect," JOSA A, vol. 22, no. 7, 1311-1318 (2005).

Distribution

2	MS 1082	Shanalyn Kemme, 1725
1	MS 1082	Robert Boye, 1725
1	MS 1082	David Peters, 1727
1	MS 1082	Jim Hudgens, 1725
1	MS 0530	Bob Nellums, 2624
1	MS 0530	Bob Habbit, 2624
2	MS 9018	Central Technical Files, 8944
2	MS 0899	Technical Library, 4536
1	MS 0123	Donna Chavez, LDRD Office, 1011